

# REPORT DOCUMENTATION PAGE

Form Approved  
OMB No. 0704-0188

Public reporting burden for this collection of information is estimated to average 1 hour per response, including the time for reviewing instructions, searching existing data sources, gathering and maintaining the data needed, and completing and reviewing this collection of information. Send comments regarding this burden estimate or any other aspect of this collection of information, including suggestions for reducing this burden to Department of Defense, Washington Headquarters Services, Directorate for Information Operations and Reports (0704-0188), 1215 Jefferson Davis Highway, Suite 1204, Arlington, VA 22202-4302. Respondents should be aware that notwithstanding any other provision of law, no person shall be subject to any penalty for failing to comply with a collection of information if it does not display a currently valid OMB control number. **PLEASE DO NOT RETURN YOUR FORM TO THE ABOVE ADDRESS.**

<b>1. REPORT DATE (DD-MM-YYYY)</b> 13 February 2003		<b>2. REPORT TYPE</b> Technical Paper		<b>3. DATES COVERED (From - To)</b>	
<b>4. TITLE AND SUBTITLE</b>  Synthesis and Characterization of the trans-IO <sub>2</sub> F <sub>5</sub> <sup>2-</sup> Dianion				<b>5a. CONTRACT NUMBER</b>	
				<b>5b. GRANT NUMBER</b>	
				<b>5c. PROGRAM ELEMENT NUMBER</b>	
<b>6. AUTHOR(S)</b>  Jerry A. Boatz, William J. Casteel, Jr., Karl O. Christe, David A. Dixon, Michael Gerken, Robert Z. Gnann, Helene P. A. Mercier, Gary J. Schrobilgen				<b>5d. PROJECT NUMBER</b> DARP	
				<b>5e. TASK NUMBER</b> A205	
				<b>5f. WORK UNIT NUMBER</b>	
<b>7. PERFORMING ORGANIZATION NAME(S) AND ADDRESS(ES)</b>  Air Force Research Laboratory (AFMC) AFRL/PRSP 10 E. Saturn Blvd. Edwards AFB, CA 93524-7680				<b>8. PERFORMING ORGANIZATION REPORT NUMBER</b>  AFRL-PR-ED-TP-2003-036	
<b>9. SPONSORING / MONITORING AGENCY NAME(S) AND ADDRESS(ES)</b>  Air Force Research Laboratory (AFMC) AFRL/PRS 5 Pollux Drive Edwards AFB CA 93524-7048				<b>10. SPONSOR/MONITOR'S ACRONYM(S)</b>	
				<b>11. SPONSOR/MONITOR'S NUMBER(S)</b> AFRL-PR-ED-TP-2003-036	
<b>12. DISTRIBUTION / AVAILABILITY STATEMENT</b>  Approved for public release; distribution unlimited.					
<b>13. SUPPLEMENTARY NOTES</b>					
<b>14. ABSTRACT</b>					
<div style="border: 1px solid black; border-radius: 15px; padding: 10px; display: inline-block;"> <span style="font-size: 2em; font-weight: bold;">20030320 049</span> </div>					
<b>15. SUBJECT TERMS</b>					
<b>16. SECURITY CLASSIFICATION OF:</b>			<b>17. LIMITATION OF ABSTRACT</b>	<b>18. NUMBER OF PAGES</b>	<b>19a. NAME OF RESPONSIBLE PERSON</b>
<b>a. REPORT</b> Unclassified	<b>b. ABSTRACT</b> Unclassified	<b>c. THIS PAGE</b> Unclassified	A		Sheila Benner
					<b>19b. TELEPHONE NUMBER (include area code)</b> (661) 275-5693

FILE

MEMORANDUM FOR PRS (In-House Publication)

FROM: PROI (STINFO)

11 Feb 2003

SUBJECT: Authorization for Release of Technical Information, Control Number: **AFRL-PR-ED-TP-2003-036**  
Jerry A. Boatz (AFRL/PRSP); William J. Casteel, Jr.; Karl O. Christe; David A. Dixon; Michael Gerken; Robert Z. Gnann; Helene P.A. Mercier, and Gary J. Schrobilgen "Synthesis and Characterization of the *trans*-IO<sub>2</sub>F<sub>3</sub><sup>2-</sup> Dianion"

55364

Journal of the American Chemical Society

(Statement A)

## Synthesis and Characterization of the *trans*-IO<sub>2</sub>F<sub>5</sub><sup>2-</sup> Dianion

Jerry A. Boatz,<sup>†</sup> William J. Casteel, Jr.,<sup>‡</sup> Karl O. Christe,<sup>†,‡,\*</sup> David A. Dixon,<sup>§</sup> Michael Gerken,<sup>‡,¶</sup> Robert Z. Gnan,<sup>‡</sup> Helene P. A. Mercier,<sup>‡</sup> and Gary J. Schrobilgen,<sup>‡,\*</sup>

*Contribution from the Loker Hydrocarbon Research Institute, University of Southern California, University Park, Los Angeles, California 90089, Air Force Research Laboratory, Edwards Air Force Base, California 93524, Department of Chemistry, McMaster University, Hamilton, Ontario L8S 4M1, Canada, and Fundamental Sciences Division, Pacific Northwest National Laboratory, Richland, Washington 99352*

### Abstract

The combination of CH<sub>3</sub>CN solutions of [N(CH<sub>3</sub>)<sub>4</sub>][F] and a mixture of *cis*- and *trans*-[N(CH<sub>3</sub>)<sub>4</sub>][IO<sub>2</sub>F<sub>4</sub>] produces the novel *trans*-IO<sub>2</sub>F<sub>5</sub><sup>2-</sup> anion. Under the given conditions, only the *trans*-IO<sub>2</sub>F<sub>4</sub><sup>-</sup> anion acts as a fluoride ion acceptor, thus allowing the separation of isomerically pure, soluble *cis*-IO<sub>2</sub>F<sub>4</sub><sup>-</sup> from insoluble *trans*-IO<sub>2</sub>F<sub>5</sub><sup>2-</sup>. The *trans*-IO<sub>2</sub>F<sub>5</sub><sup>2-</sup> and *cis*-IO<sub>2</sub>F<sub>4</sub><sup>-</sup> anions were characterized by infrared and Raman spectroscopy and theoretical calculations at the LDFT and HF levels of theory. The *trans*-IO<sub>2</sub>F<sub>5</sub><sup>2-</sup> anion has a pentagonal-bipyramidal geometry with the two oxygen atoms occupying the axial positions. It represents the first example of a heptacoordinated main group AO<sub>2</sub>X<sub>5</sub> species and completes the series of pentagonal-bipyramidal iodine fluoride and oxofluoride species. The geometries of the pentagonal-bipyramidal series IO<sub>2</sub>F<sub>5</sub><sup>2-</sup>, IOF<sub>5</sub><sup>2-</sup>, IF<sub>5</sub><sup>2-</sup>, IOF<sub>6</sub><sup>-</sup>, IF<sub>6</sub><sup>-</sup>, and IF<sub>7</sub>, and the corresponding octahedral series IO<sub>2</sub>F<sub>4</sub><sup>-</sup>, IOF<sub>4</sub><sup>-</sup>, IF<sub>4</sub><sup>-</sup>, IOF<sub>5</sub>, IF<sub>5</sub>, and IF<sub>6</sub><sup>+</sup> were calculated by identical methods. It is shown how the ionic charge, the oxidation state of the central atom, the coordination number, and the replacement of fluorine ligands by either an oxygen ligand or a free valence electron pair influence the structures and bonding of these species.

**DISTRIBUTION STATEMENT A**  
Approved for Public Release  
Distribution Unlimited

## Introduction

Main-group fluorides and oxofluorides offer a unique opportunity to study high coordination numbers, the steric influence and relative repulsion effects of fluorine, oxygen and sterically active free valence electron pairs, and fluxionality. Of particular interest in this respect is the coordination number seven. Although heptacoordinated species can exist in three different conformations of similar energy, i. e., either as a monocapped octahedron, a monocapped trigonal prism, or a pentagonal bipyramid,<sup>1,2</sup> main group elements generally prefer pentagonal bipyramidal structures<sup>3,4</sup> since this geometry results in a better overlap of the ligand orbitals with the *s* and *p* orbitals of the central atom. As part of our systematic studies of heptacoordination, the structures of main group  $AF_5XY$  species have been studied where X and Y represent either fluorine or oxygen ligands or sterically active free valence electron pairs (E).<sup>3,5-14</sup> Structures for all members of this series have been established, except for the  $AO_2F_5$  case. In this paper, the preparation and structure of the  $IO_2F_5^{2-}$  dianion, the first example of a main-group  $AO_2F_5$  species, is reported.

## Experimental

**Materials and Apparatus.** All volatile materials were handled in either a Pyrex vacuum line equipped with Kontes or J. Young glass-Teflon valves or a stainless steel, Teflon-FEP vacuum line.<sup>15</sup> Nonvolatile materials were handled in the dry nitrogen atmosphere of a glove box.

The solvents,  $CH_3CN$  (Baker, HPLC Grade) and anhydrous HF (Harshaw) were dried by storage over  $P_2O_5$  and  $BiF_5$ ,<sup>16</sup> respectively, and distilled prior to their use. The syntheses of  $[N(CH_3)_4][F]^{17}$  and  $IO_2F_3^{18}$  have been described previously.

**Preparation of  $[N(CH_3)_4][IO_4]$ .** Tetramethylammonium metaperiodate,  $[N(CH_3)_4][IO_4]$ , was prepared either by a literature method<sup>19</sup> or by the following metathesis reaction. Approximately 30 mL of a 0.76 M aqueous solution of  $[N(CH_3)_4][Cl]$  (Fluka Chemika, 98%)

(22.80 mmol) was slowly added, with stirring, to 40 mL of aqueous  $[\text{Na}][\text{IO}_4]$  (Matheson Coleman & Bell, 99.8%) (22.77 mmol). A white precipitate formed almost immediately and the resulting mixture was stirred in an ice water bath for 30 min. The  $[\text{N}(\text{CH}_3)_4][\text{IO}_4]$  precipitate was filtered off, washed with ice cold water, and dried for 15 h at 88 °C in a dynamic vacuum.  $[\text{N}(\text{CH}_3)_4][\text{IO}_4]$  was obtained in a yield of 53.7 % (3.2643 g). Infrared and Raman spectroscopy of the product showed no detectable amounts of water.

**Preparation of  $[\text{N}(\text{CH}_3)_4][\text{IO}_2\text{F}_4]$ .** Tetramethylammonium tetrafluoroperiodate was prepared by analogy with a previously published<sup>20</sup> method. In the drybox,  $[\text{N}(\text{CH}_3)_4][\text{IO}_4]$  (2.995 mmol) was loaded into a 20 cm long, 1/2-in. o.d. Teflon-FEP tube that was closed by a Kel-F valve. On the metal line, anhydrous HF (3.4 mL) was distilled onto the  $[\text{N}(\text{CH}_3)_4][\text{IO}_4]$ . The mixture was allowed to warm to room temperature, giving a colorless solution, and agitated for 3 days on a mechanical shaker. The HF and  $\text{H}_2\text{O}$  were pumped off between 0 °C and 45 °C for 14 h. Fresh anhydrous HF was distilled onto the sample and the tube was agitated for an additional 2 days, followed by removal of the solvent in a dynamic vacuum to give  $[\text{N}(\text{CH}_3)_4][\text{IO}_2\text{F}_4]$  in 96.8% yield in the form of a white, crystalline solid. The purity was verified by its low-temperature Raman spectrum, which showed the presence of a mixture of  $[\text{N}(\text{CH}_3)_4][\text{cis-IO}_2\text{F}_4]$  and  $[\text{N}(\text{CH}_3)_4][\text{trans-IO}_2\text{F}_4]$  (*cis-IO*<sub>2</sub>F<sub>4</sub><sup>-</sup>: 207 (3), 235 (<0.5), 330 (35), 366 sh, 394 (19),  $\nu_4(\text{A}_1)$ ; 560 (24),  $\nu_3(\text{A}_1)$ ; 610 (74),  $\nu_2(\text{A}_1)$ ; 847 (75),  $\nu_1(\text{A}_1)$ ; and 870 (13), 880 sh,  $\text{cm}^{-1}$ ,  $\nu_{12}(\text{B}_2)$ ; *trans-IO*<sub>2</sub>F<sub>4</sub><sup>-</sup>: 251 (5),  $\nu_6(\text{B}_{2g})$ ; 380 (41),  $\nu_8(\text{E}_g)$ ; 560 (24),  $\nu_5(\text{B}_{1g})$ ; 571 (65),  $\nu_2(\text{A}_{1g})$ ; and 813 (100)  $\text{cm}^{-1}$ ,  $\nu_1(\text{A}_{1g})$ ). Fluorine-19 NMR spectroscopy of  $[\text{N}(\text{CH}_3)_4][\text{IO}_2\text{F}_4]$  in HF solution indicated an approximate *cis-* to *trans-* isomer ratio of 70:30.

Alternatively,  $[\text{N}(\text{CH}_3)_4][\text{IO}_2\text{F}_4]$  was prepared from  $\text{IO}_2\text{F}_3$  and  $[\text{N}(\text{CH}_3)_4][\text{F}]$ . In a typical synthesis,  $\text{IO}_2\text{F}_3$  (10.774 mmol) was condensed into a 3/8-in. o.d. Teflon-FEP reaction tube equipped with a Kel-F valve, and 5 mL of anhydrous HF was condensed onto the solid at -196

°C. The  $\text{IO}_2\text{F}_3$  completely dissolved upon warming to room temperature and agitation. The solution was transferred into a drybox and frozen in a  $-196$  °C cold well, and  $[\text{N}(\text{CH}_3)_4][\text{F}]$  (11.050 mmol) was added. The reactor was removed from the drybox and warmed to room temperature resulting in a colorless solution. Removal of the HF for several hours in a dynamic vacuum gave colorless, friable, microcrystalline  $[\text{N}(\text{CH}_3)_4][\text{IO}_2\text{F}_4]$  (10.854 mmol). Its purity was established by Raman spectroscopy. **CAUTION: The condensation of  $\text{IO}_2\text{F}_3$  onto frozen  $\text{CH}_3\text{CN}$  solutions can result in detonations when the mixtures are warmed to the melting point of the solvent and must be avoided.**

**Preparation of  $[\text{N}(\text{CH}_3)_4]_2[\text{IO}_2\text{F}_5]$ .** Inside the drybox,  $[\text{N}(\text{CH}_3)_4][\text{IO}_2\text{F}_4]$  (1.853 mmol) was added to one arm of a flamed-out, H-shaped glass reaction vessel equipped with a Young valve on each side and one separating the two arms. A stoichiometric amount of  $[\text{N}(\text{CH}_3)_4][\text{F}]$  (1.882 mmol) was added to the other arm of the reaction vessel. Anhydrous  $\text{CH}_3\text{CN}$  was condensed at  $-196$  °C into both arms, and the reactor was warmed to  $-30$  °C. The  $\text{CH}_3\text{CN}$  solution of  $[\text{N}(\text{CH}_3)_4][\text{F}]$  was transferred into the arm of the reaction vessel containing the  $[\text{N}(\text{CH}_3)_4][\text{IO}_2\text{F}_4]$  solution. The mixture was stirred at  $-30$  °C for 2 h using a magnetic stir bar. The  $\text{CH}_3\text{CN}$  solvent was pumped off over a period of 16 h while slowly warming from  $-30$  to  $0$  °C, yielding 0.7970 g of a fine, white powder consisting of  $[\text{N}(\text{CH}_3)_4]_2[\text{IO}_2\text{F}_5]$ ,  $[\text{N}(\text{CH}_3)_4][\text{F}]$ , and  $[\text{N}(\text{CH}_3)_4][\text{cis-IO}_2\text{F}_4]$ .

Inside the drybox, part of the above described  $[\text{N}(\text{CH}_3)_4]_2[\text{IO}_2\text{F}_5]$  /  $[\text{N}(\text{CH}_3)_4][\text{F}]$  /  $[\text{N}(\text{CH}_3)_4][\text{cis-IO}_2\text{F}_4]$  mixture (0.3433 g) was loaded into one arm of the H-shaped reaction vessel. Anhydrous  $\text{CH}_3\text{CN}$  was distilled onto the mixture in a static vacuum at  $-196$  °C. The mixture was allowed to warm to  $-20$  °C, was agitated, and then allowed to settle. After 2 h, the  $\text{CH}_3\text{CN}$  solution was decanted into the other arm of the reaction vessel, and the solvent was distilled back onto the solid residue. Washing of the solid was repeated ten more times before the  $\text{CH}_3\text{CN}$  solvent was

pumped off on the glass vacuum line for 12 h while warming from -30 to 25 °C to yield 0.1382 g of a fine, white powder that consisted, based on its weight and vibrational spectra, of 75 weight %  $[\text{N}(\text{CH}_3)_4]_2[\text{IO}_2\text{F}_5]$  and 25 weight %  $[\text{N}(\text{CH}_3)_4][\text{cis-IO}_2\text{F}_4]$ .

Alternatively, a previously described Teflon-FEP metathesis apparatus<sup>21</sup> was loaded in the dry box with  $[\text{N}(\text{CH}_3)_4][\text{F}]$  (2.58 mmol) and  $[\text{N}(\text{CH}_3)_4][\text{IO}_2\text{F}_4]$  (2.01 mmol). On a glass vacuum line, approximately 10 mL  $\text{CH}_3\text{CN}$  was condensed onto the solid at -196 °C. After melting of the  $\text{CH}_3\text{CN}$  solvent at -31 °C, the reaction mixture was kept at -31 °C for 2 h and periodically stirred resulting in the formation of copious amounts of white solid. The apparatus was inverted and the reaction mixture was quickly pressure filtered, followed by removal of the  $\text{CH}_3\text{CN}$  in a dynamic vacuum at ambient temperature. Inside the dry box, the apparatus was disassembled and 0.550 g of a white solid from the filter cake (containing  $[\text{N}(\text{CH}_3)_4]_2[\text{IO}_2\text{F}_5]$ ,  $[\text{N}(\text{CH}_3)_4][\text{cis-IO}_2\text{F}_4]$ , and trace amounts of  $[\text{N}(\text{CH}_3)_4][\text{trans-IO}_2\text{F}_4]$ ) and 0.250 g of a white filtrate residue, containing  $[\text{N}(\text{CH}_3)_4][\text{F}]$  and isomerically pure  $[\text{N}(\text{CH}_3)_4][\text{cis-IO}_2\text{F}_4]$ , were collected.

In another modification, clear solutions of  $[\text{N}(\text{CH}_3)_4][\text{F}]$  (2.90 mmol) in 15 mL  $\text{CH}_3\text{CN}$  and  $[\text{N}(\text{CH}_3)_4][\text{IO}_2\text{F}_4]$  (2.04 mmol) in 7 mL  $\text{CH}_3\text{CN}$  were combined inside a dry box in a 100 mL Teflon bottle. Instantaneously, a copious white precipitate formed that was pressure-filtered through a Teflon filter (Pall Corp). The white filtercake was transferred into a 3/4" o.d. Teflon ampoule equipped with a stainless steel valve and pumped to dryness for 2 h at ambient temperature. Vibrational spectroscopy of the filtercake showed the presence of  $[\text{N}(\text{CH}_3)_4]_2[\text{IO}_2\text{F}_5]$ ,  $[\text{N}(\text{CH}_3)_4][\text{cis-IO}_2\text{F}_4]$ , and trace amounts of  $[\text{N}(\text{CH}_3)_4][\text{trans-IO}_2\text{F}_4]$ .

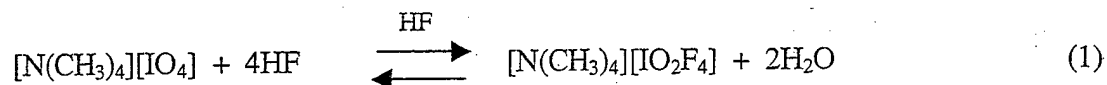
**Raman Spectroscopy.** The low-temperature spectra were recorded either with a Jobin-Yvon Model S-3000 spectrometer, using the 514.5 nm line of an Ar ion laser and an Olympus metallurgical microscope (model BHSM-L-2) for focusing the laser, a Cary Model 83GT with 488 nm excitation from an Ar ion laser, or a Spex Model 1403 with 647.1 nm excitation from a

Kr ion laser. Spectra were recorded at low temperature using microcrystalline samples of  $[\text{N}(\text{CH}_3)_4]_2[\text{IO}_2\text{F}_5]$  /  $[\text{N}(\text{CH}_3)_4][\text{cis-IO}_2\text{F}_4]$  sealed in Pyrex melting point capillaries.

**Theoretical Calculations.** Electronic structure calculations were done at the local density functional theory (LDFT)<sup>22,23</sup> and the Hartree-Fock (HF) level.<sup>24</sup> The LDFT calculations were done with a polarized valence double  $\zeta$  basis set (DZVP).<sup>25</sup> The HF calculations were done with a polarized valence double  $\zeta$  basis set augmented by diffuse functions<sup>26</sup> on O and F and a polarized valence double  $\zeta$  basis set on I with an effective core potential.<sup>27</sup> Geometries were optimized and second derivatives were calculated at the optimized geometries. The initial LDFT calculations were done with DGauss<sup>28</sup> (using the A1 charge fitting basis set) and the final LDFT and HF calculations were done with Gaussian 98.<sup>29</sup> The second derivatives were analyzed by using the program BMATRIX developed by Komornicki.<sup>30</sup> Raman intensities were determined analytically at the HF level and numerically at the LDFT level. Because we did not use a large basis set with diffuse functions to get accurate polarizabilities, the Raman intensities provide only qualitative information.

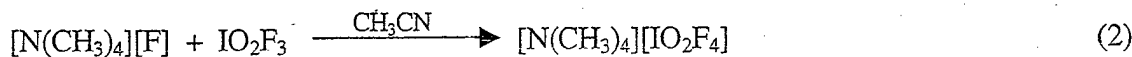
## Results and Discussion

**Synthesis of  $[\text{N}(\text{CH}_3)_4][\text{IO}_2\text{F}_4]$ .** The  $\text{N}(\text{CH}_3)_4^+$  salt of the known  $\text{IO}_2\text{F}_4^-$  anion was prepared by two synthetic routes. In analogy to the reported preparation of  $[\text{Cs}][\text{IO}_2\text{F}_4]$ ,<sup>20</sup> a mixture of *cis*- and *trans*-  $[\text{N}(\text{CH}_3)_4][\text{IO}_2\text{F}_4]$  in a 7 : 3 isomer ratio was obtained from  $[\text{N}(\text{CH}_3)_4][\text{IO}_4]$  upon repeated treatments with a large excess of anhydrous HF (eq(1)).

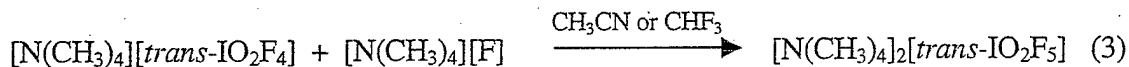


Alternatively,  $[\text{N}(\text{CH}_3)_4][\text{IO}_2\text{F}_4]$  was synthesized by the reaction of  $\text{IO}_2\text{F}_3$  with  $[\text{N}(\text{CH}_3)_4][\text{F}]$  in

CH<sub>3</sub>CN solution (eq (2)).



**Synthesis of [N(CH<sub>3</sub>)<sub>4</sub>]<sub>2</sub>[IO<sub>2</sub>F<sub>5</sub>].** A mixture of *cis*- and *trans*- [N(CH<sub>3</sub>)<sub>4</sub>][IO<sub>2</sub>F<sub>4</sub>] was allowed to react with one mole equivalent of [N(CH<sub>3</sub>)<sub>4</sub>][F] in CH<sub>3</sub>CN either at -30 °C or at ambient temperature. The solvent was pumped off in a dynamic vacuum, yielding a white product consisting of [N(CH<sub>3</sub>)<sub>4</sub>]<sub>2</sub>[*trans*-IO<sub>2</sub>F<sub>5</sub>] and [N(CH<sub>3</sub>)<sub>4</sub>][*cis*-IO<sub>2</sub>F<sub>4</sub>]. The reaction was also carried out in CHF<sub>3</sub> solution at 0 °C, but is less convenient due to the high vapor pressure of the solvent and the presence of some unreacted [N(CH<sub>3</sub>)<sub>4</sub>][*trans*-IO<sub>2</sub>F<sub>4</sub>] in the product. These results show that under the given reaction conditions only *trans*-IO<sub>2</sub>F<sub>4</sub><sup>-</sup> reacts with F<sup>-</sup>, yielding the *trans*-IO<sub>2</sub>F<sub>5</sub><sup>2-</sup> anion according to eq. (3).



The observation that exclusively the *trans*-IO<sub>2</sub>F<sub>4</sub><sup>-</sup> ion reacts with the F<sup>-</sup> ion can be rationalized by kinetic effects. Because the oxygen double bond domains are larger and more repulsive than those of the fluorine single bonds,<sup>2,31</sup> the F<sup>-</sup> ion approaches the IO<sub>2</sub>F<sub>4</sub><sup>-</sup> ion in the direction of the least repulsion, i.e., through a triangular F<sub>3</sub> face in *cis*-IO<sub>2</sub>F<sub>4</sub><sup>-</sup>, and through an F<sub>2</sub>O face in *trans*-IO<sub>2</sub>F<sub>4</sub><sup>-</sup>. In the latter case, the additional fluorine ligand can easily slip into the existing equatorial fluorine belt, resulting directly in the energetically favored *trans*-IO<sub>2</sub>F<sub>5</sub><sup>2-</sup> structure of *D*<sub>5h</sub> symmetry. In the case of *cis*-IO<sub>2</sub>F<sub>4</sub><sup>-</sup>, however, the analogous approach results in an intermediate structure that cannot easily rearrange to *D*<sub>5h</sub> symmetry without the kinetically unfavorable, complete breakage and reformation of an I-F bond. This type of argument can also explain the lack of easy *cis/trans*-isomerization in pseudo-octahedral species, such as IO<sub>2</sub>F<sub>4</sub><sup>-</sup>, and the ease of this isomerization in pseudo trigonal-bipyramidal species through a Berry pseudorotation mechanism.<sup>32</sup>

Although most of the unreacted [N(CH<sub>3</sub>)<sub>4</sub>][*cis*-IO<sub>2</sub>F<sub>4</sub>] salt can be extracted from the

product mixture using  $\text{CH}_3\text{CN}$ , not all of the  $[\text{N}(\text{CH}_3)_4][\text{cis-IO}_2\text{F}_4]$  was removed even after numerous washings. Removal of the solvent from the washings afforded isomerically pure  $[\text{N}(\text{CH}_3)_4][\text{cis-IO}_2\text{F}_4]$ , containing only some  $[\text{N}(\text{CH}_3)_4][\text{F}]$ , as shown by infrared spectroscopy. Although isomerically pure *trans*- $\text{IO}_2\text{F}_4^-$  had previously been prepared,<sup>33</sup> this procedure represents the first isolation of isomerically pure *cis*- $\text{IO}_2\text{F}_4^-$ .

Attempts to grow single crystals of  $[\text{N}(\text{CH}_3)_4][\text{cis-IO}_2\text{F}_4]$  from the  $\text{CH}_3\text{CN}$  extract of the crude  $[\text{N}(\text{CH}_3)_4]_2[\text{IO}_2\text{F}_5] / [\text{N}(\text{CH}_3)_4][\text{cis-IO}_2\text{F}_4] / [\text{N}(\text{CH}_3)_4][\text{F}]$  reaction product yielded crystals of  $[\text{N}(\text{CH}_3)_4]_2[\text{IO}_2\text{F}_2][\text{HF}_2]$  instead.<sup>34</sup> The reducing agent required for the reduction of  $\text{I}(\text{VII})\text{O}_2\text{F}_4^-$  to  $\text{I}(\text{V})\text{O}_2\text{F}_2^-$  is most likely  $\text{CH}_3\text{CN}$ . Tetramethylammonium fluoride may play a crucial role in this reduction because it is known to readily abstract a proton from  $\text{CH}_3\text{CN}$  yielding the  $\text{CH}_2\text{CN}^-$  anion.<sup>17</sup>

**Vibrational Spectra and Structure of the *trans*- $\text{IO}_2\text{F}_5^{2-}$  Anion.** The Raman spectrum of  $[\text{N}(\text{CH}_3)_4]_2[\text{IO}_2\text{F}_5]$  containing about 25 weight % of  $[\text{N}(\text{CH}_3)_4][\text{cis-IO}_2\text{F}_4]$  is shown in Figure 1. The observed vibrational frequencies for  $\text{IO}_2\text{F}_5^{2-}$  and their assignments based on the theoretical calculations are summarized in Table 1. After subtraction of the bands belonging to the  $\text{N}(\text{CH}_3)_4^+$  cation,<sup>35</sup> the *cis*- $\text{IO}_2\text{F}_4^-$  anion, and trace amounts of  $\text{CH}_3\text{CN}$ , four new Raman bands at 789, 517, 395, and 368  $\text{cm}^{-1}$  and four new infrared bands at 847, 490, 390, and 330  $\text{cm}^{-1}$  remain that can be assigned to the novel pentagonal-bipyramidal  $\text{IO}_2\text{F}_5^{2-}$  anion of  $D_{5h}$  symmetry with the oxygen atoms in the two axial positions (see Figure 2).

A total of 18 vibrational modes are expected for the  $\text{IO}_2\text{F}_5^{2-}$  anion of  $D_{5h}$  symmetry which span the irreducible representations  $\Gamma = 2A_1' + 3E_1' + 2E_2' + 2A_2'' + E_1'' + E_2''$ . Of the resulting 11 fundamental vibrations, five are Raman active ( $2A_1'$ ,  $2E_2'$ , and  $E_1''$ ), five are infrared active ( $2A_2''$  and  $3E_1'$ ), and the  $E_2''$  mode is inactive. Of the expected five Raman and five infrared active vibrations, four were observed in each spectrum. The Raman band at 789 and the infrared band at 847  $\text{cm}^{-1}$  represent the symmetric ( $\nu_1(A_1')$ ) and antisymmetric ( $\nu_3(A_2'')$ ) stretching modes of the axial  $\text{IO}_2$  unit, respectively. Their large frequency separation and mutual exclusion establish beyond doubt the linearity, i.e., the *trans*-configuration, of the O-I-O group. For the *cis*-

configuration and the monocapped octahedral and monocapped trigonal prismatic geometries, the symmetric and the antisymmetric  $\text{IO}_2$  stretching modes would be both Raman and infrared active. This conclusion is further supported by a comparison with the spectra of  $\text{trans-IO}_2\text{F}_4^-$  in its  $\text{N}(\text{CH}_3)_4^+$  salt, where the mutually exclusive  $\text{IO}_2$  stretching modes were observed at 813 and 880  $\text{cm}^{-1}$ .<sup>20</sup> The observed decreases in frequency from  $\text{IO}_2\text{F}_4^-$  to  $\text{IO}_2\text{F}_5^{2-}$  are consistent with the greater I-O bond polarity in the  $\text{IO}_2\text{F}_5^{2-}$  anion resulting from the increased negative formal charge in the dianion (see below).

Similarly, the Raman band at 517  $\text{cm}^{-1}$ , which corresponds to the symmetric stretching mode,  $\nu_2(\text{A}_1')$ , of the five equatorial I-F bonds, is considerably lower in frequency than the corresponding band found at 571  $\text{cm}^{-1}$  for the four I-F bonds in  $\text{trans-IO}_2\text{F}_4^-$ . The second Raman active  $\text{IF}_5$  stretching mode,  $\nu_9(\text{E}_2')$ , was not observed because of its low intensity and interference with the 457  $\text{cm}^{-1}$  band of  $\text{N}(\text{CH}_3)_4^+$ . The infrared active antisymmetric  $\text{IF}_5$  stretching mode,  $\nu_5(\text{E}_1')$ , was observed as a very strong IR band at 490  $\text{cm}^{-1}$ , in accord with the predicted frequency and intensity values. The Raman band at 368  $\text{cm}^{-1}$  is assigned to the  $\text{IO}_2$  rocking mode,  $\nu_8(\text{E}_1'')$ , of  $\text{IO}_2\text{F}_5^{2-}$ , in accord with its predicted frequency and high Raman intensity.<sup>11,12</sup> The only remaining Raman band occurs at 395  $\text{cm}^{-1}$ , in excellent agreement with the frequency predictions for the  $\text{IF}_5$  scissoring mode,  $\nu_{10}(\text{E}_2')$ . Of the three expected infrared active deformation modes, the  $\text{IO}_2$  scissoring mode,  $\nu_6(\text{E}_1')$ , and the  $\text{IF}_5$  umbrella deformation mode,  $\nu_4(\text{A}'')$ , were observed at the expected frequencies. The remaining antisymmetric  $\text{IF}_5$  in plane deformation mode,  $\nu_7(\text{E}_1')$ , was not observed because of its low frequency and predicted near zero infrared intensity. The observed vibrational spectra are in excellent agreement with the qualitative predictions and calculated frequencies for  $\text{trans-IO}_2\text{F}_5^{2-}$  of  $D_{5h}$  symmetry and confirm the existence and symmetry of this novel anion beyond doubt.

The pentagonal-bipyramidal  $D_{5h}$  geometry of  $\text{IO}_2\text{F}_5^{2-}$  is in accord with the VSEPR models<sup>2</sup> and with the structures previously established for  $\text{IF}_5^{2-}$  and  $\text{IOF}_5^{2-}$ .<sup>10,14</sup> All three anions possess a pentagonal  $\text{IF}_5$  plane with the two axial positions occupied by free valence electron pairs or oxygen atoms. This is in accord with the doubly bonded oxygen and the free valence electron pair domains

being more repulsive than those of the fluorine ligands<sup>2</sup> and, therefore, occupying the less crowded axial positions. In this manner, they achieve maximum avoidance.

It is interesting to examine the frequency trends for the pentagonal planar  $\text{IF}_5$  group within the  $\text{IF}_7$ ,  $\text{IOF}_6^-$ ,  $\text{IO}_2\text{F}_5^{2-}$ ,  $\text{IOF}_5^{2-}$ , and  $\text{IF}_5^{2-}$  series. In the isoelectronic  $\text{IF}_7$ ,  $\text{IOF}_6^-$ , and  $\text{IO}_2\text{F}_5^{2-}$  sequence, the oxidation state of iodine remains the same (+VII), whereas the axial fluorine ligands are stepwise replaced by formally negatively charged O ligands thereby increasing the overall negative charges. In the  $\text{IO}_2\text{F}_5^{2-}$ ,  $\text{IOF}_5^{2-}$ , and  $\text{IF}_5^{2-}$  sequence, the axial oxygen ligands are stepwise replaced by free valence electron pairs, causing a stepwise reduction of the iodine oxidation state from +VII to +III.

As shown in Table 2, the  $\text{IF}_5$  stretching modes are most strongly influenced by the ionic charges and the resulting polarity of the I-F bonds, and to a lesser extent by the replacement of oxygen by a free valence electron pair. Similarly, the  $\text{IF}_5$  in-plane deformation frequencies decrease with an increase in the ionic charge, but change only little upon replacement of an oxygen ligand by a free valence electron pair, especially for the replacement of the second oxygen atom by a free valence electron pair. The out-of-plane deformation modes change much less. Apparently, the lengthening and weakening of the I-F bonds by their increasing polarity is counteracted by the increased repulsion resulting from the replacement of an axial fluorine ligand by either a more repelling oxygen ligand or an iodine free valence electron pair.

Although no main group  $D_{5h}$   $\text{AO}_2\text{X}_5$  species had previously been reported, the crystal structure<sup>36</sup> and infrared spectrum<sup>37</sup> of pentagonal-bipyramidal  $\text{UO}_2\text{F}_5^{3-}$  were published in 1954 and 1968, respectively. A comparison of the vibrational frequencies and assignments listed<sup>38</sup> for  $\text{UO}_2\text{F}_5^{3-}$  with those of *trans*- $\text{IO}_2\text{F}_5^{2-}$  casts serious doubts on the published vibrational analysis of  $\text{UO}_2\text{F}_5^{3-}$ . Particularly disturbing are the high frequencies attributed to the U-F stretching modes in this trianion.

**Vibrational Spectra of  $[\text{N}(\text{CH}_3)_4][\text{cis-IO}_2\text{F}_4]$ .** The availability of isomerically pure  $[\text{N}(\text{CH}_3)_4][\text{cis-IO}_2\text{F}_4]$ , of previous data for the isomerically impure cesium salt,<sup>20</sup> and of calculated frequencies and intensities permitted conclusive assignments for this anion (see Table 3). With the

exception of  $\nu_6$  and  $\nu_{15}$ , which based on the theoretical predictions have vanishing infrared and Raman intensities, all fundamental vibrations can be assigned to the experimentally observed frequencies, assuming double coincidences for  $\nu_5 / \nu_{14}$  and  $\nu_7 / \nu_{11}$ , respectively. This assumption is supported by the theoretical calculations which predict that their frequencies are almost identical. The observed spectra are in accord with the theoretical predictions and those of the closely related *cis*-OsO<sub>2</sub>F<sub>4</sub> molecule<sup>39</sup> which exhibits a very similar spectrum. The following geometry was calculated for *cis*-IO<sub>2</sub>F<sub>4</sub><sup>-</sup> at the HF/ECP/DZVP level of theory: I-O 1.731 Å; I-F<sub>ax</sub> = 1.843 Å; I-F<sub>eq</sub> = 1.856 Å; O-I-O = 104.4 °; O-I-F<sub>ax</sub> = 95.3 °; O-I-F<sub>eq</sub> = 89.3 °; F<sub>eq</sub>-I-F<sub>eq</sub> = 77.0 °; with the energy of the *cis*-isomer being 3.3 kcal/mol, 2.3 kcal/mol, and 1.8 kcal/mol higher than that of the *trans*-isomer at the HF/ECP, NLDFT, and LDFT levels of theory, respectively. The I-O and I-F bond lengths in the *cis*-isomer are very similar to those (I-O = 1.731 Å and I-F = 1.855 Å) of the *trans*-isomer at the same level of theory.

### Theoretical Calculations

**Normal Coordinate Analysis of *trans*-IO<sub>2</sub>F<sub>5</sub><sup>2-</sup>.** Because doubly charged anions, such as IO<sub>2</sub>F<sub>5</sub><sup>2-</sup>, exhibit only very little solubility in common solvents and, in solution, revert to the singly charged anions and free fluoride, it was not possible to grow single crystals for x-ray diffraction. Therefore, theoretical calculations of the vibrational frequencies and intensities and their fit with the observed spectra were used to determine the structure of IO<sub>2</sub>F<sub>5</sub><sup>2-</sup> and to evaluate the structural trends resulting from changes in the formal ionic charge, the oxidation state and coordination number (CN) of iodine, and the replacement of an oxygen ligand by either a free valence electron pair or a fluorine ligand. Because our previous work had shown that for closely related iodine and xenon compounds HF/ECP/DZVP and LDFT/DZVP calculations, after appropriate scaling, approximate the experimental values quite well, the same approach was chosen for the present study.

As shown in Table 1, the agreement between the observed and calculated frequencies and intensities is good for IO<sub>2</sub>F<sub>5</sub><sup>2-</sup>, thus confirming its *D*<sub>5h</sub> geometry (see Figure 2). Based on a general

comparison of calculated and experimental geometries for the closely related six-coordinated series  $\text{IO}_2\text{F}_4^-$ ,  $\text{IOF}_4^-$ ,  $\text{IF}_4^-$ ,  $\text{IOF}_5$ ,  $\text{IF}_5$ , and  $\text{IF}_6^+$  and the seven-coordinated series  $\text{IO}_2\text{F}_5^{2-}$ ,  $\text{IOF}_5^{2-}$ ,  $\text{IF}_5^{2-}$ ,  $\text{IOF}_6^-$ ,  $\text{IF}_6^-$ , and  $\text{IF}_7$  (see Figures 3 and 4, respectively), the following bond lengths are predicted for *trans*- $\text{IO}_2\text{F}_5^{2-}$ :  $r_{\text{I-F}} = 1.97 \text{ \AA}$  and  $r_{\text{I-O}} = 1.78 \text{ \AA}$  (see Table 4).

In view of the importance of the vibrational spectra for the identification of the novel *trans*- $\text{IO}_2\text{F}_5^{2-}$  anion, a normal coordinate analysis was carried out using the scaled LDFT/DZVP frequencies from Table 1. The results are summarized in Table 5 and confirm the assignments and approximate mode descriptions given in Table 1. As can be seen from the Potential Energy Distribution (PED) in Table 5, all modes are highly characteristic, except for  $\nu_6$  and  $\nu_7$  which are symmetric and antisymmetric combinations, respectively, of the  $\text{IO}_2$  scissoring and the  $\text{IF}_5$  antisymmetric in plane deformation motions. The I-O and I-F stretching force constants have values of about  $5.64 \text{ mdyn/\AA}$  and  $2.42 \text{ mdyn/\AA}$ , respectively, and correlate well with the predicted bond distances.

**Analysis of *cis*- $\text{IO}_2\text{F}_5^{2-}$ .** The stability of *cis*-isomers of  $\text{IO}_2\text{F}_5^{2-}$  was also explored computationally at the LDFT/dzvp level of theory. Only one stable isomer was found which is shown in Figure 5. It possesses one axial and one equatorial oxygen atom and is 19.6 kcal/mol higher in energy than the *trans*-isomer. The equatorial oxygen ligand requires more space than the fluorine ligands and is displaced from the equatorial plane by about  $20^\circ$ . This displacement causes a tilt of the adjacent axial fluorine ligand by about  $14^\circ$ . The remaining  $\text{F}_{\text{ax}}\text{IF}_4$  fragment of the ion is part of an almost perfect pentagonal bipyramid. The geometry and unscaled vibrational frequencies of the *cis*-isomer of  $\text{IO}_2\text{F}_5^{2-}$  are summarized in Table 6. The poor correspondence between calculated and observed frequencies and intensities rules out the possibility of assigning the observed spectra to the *trans*-isomer.

**General Trends.** Figures 3 and 4 also allow us to study the influence of the coordination number and oxidation state of iodine and of the ionic charge on the structures of these species. Because the HF/ECP/DZVP bond lengths approximate the experimental values better than the LDFT/DZVP results, the former values were used. In spite of  $\text{IF}_6^-$  having in its  $\text{N}(\text{CH}_3)_4^+$  salt a

monocapped octahedral structure,<sup>40</sup> a pseudopentagonal-bipyramidal structure was used for our study to allow a better comparison with the other members of this series. This is not unreasonable because the three possible structures, a monocapped octahedron, a pentagonal bipyramid, and a monocapped trigonal prism are very close in energy,<sup>1,41</sup>

An analysis of these figures reveals the following effects.

(i): The hexa- and hepta-coordinated compounds exhibit similar general trends, except for the bonds in the hepta-coordinated compounds being longer than those in the hexa-coordinated ones. Whereas this difference is very pronounced for the equatorial iodine-fluorine bonds (~8-10 pm), it is much smaller (~1-2 pm) for the other bonds. Because in these two series the equatorial fluorine ligands preferentially form semi-ionic, multi-center bonds,<sup>9,42-44</sup> they are much more susceptible to changes induced by hypervalency and increased bond ionicity.

(ii): The equatorial I-F bond lengths are most strongly influenced by the ionic charges of the ions and the oxidation state of the central iodine atom (see Figure 6). This is not surprising in view of Statement (i), because both, an increased negative charge and a reduced effective electronegativity of the central atom, increase the ionicity of the equatorial I-F bonds.

(iii): The axial I-F bonds are predominantly covalent and, therefore, similar in the hexa- and hepta-coordinated species. They also gain substantial ionicity from an increase in the ion charge (see Figure 7).

(iv): The axial I-O bonds are also similar in the hexa- and hepta-coordinated species, but are much less influenced by changes in either the ion charge or the oxidation state of the central atom (see Figure 8).

(v): As one might expect, the replacement of axial fluorine ligands by less electron withdrawing oxygen ligands and the replacement of oxygen ligands by electron feeding free valence electron pairs both decrease the effective electronegativity of the central atom and, thereby, increase the ionicity of the remaining I-F bonds. However, because these changes always go hand-in-hand with changes in the ion charge and the oxidation state of the central atom, they cannot be assessed independently in a more quantitative manner. The combination of these effects causes

$\text{IF}_6^+$ , with a positive ion charge, an iodine oxidation state of (VII), a CN of six, and no oxygen ligands or free iodine valence electron pairs, to exhibit the shortest I-F bond (1.75 Å), while  $\text{IF}_5^{2-}$ , with two negative ion charges, an iodine oxidation state of (III), a CN of seven, and two free iodine valence electron pairs, has the longest I-F bonds of 2.095 Å. This wide range in the I-F bond lengths is quite remarkable.

(vi): The O-I-F bond angles in  $\text{IOF}_4^-$  and  $\text{IOF}_5^{2-}$ , which contain one oxygen atom and one free valence electron pair in the two axial positions, provide information concerning the relative repulsion domains of doubly bonded oxygen and a sterically active free valence electron pair. In both ions, the O-I-F angle is somewhat larger than  $90^\circ$ , indicating that, in these compounds, the doubly bonded oxygen domain is slightly more repulsive than that of the free valence electron pair.

(vii): The experimentally observed bond distances (see Figures 3 and 4) are in accord with the calculated trends except for the axial I-F bond reported for  $\text{IOF}_5$ .<sup>45</sup> The reported electron diffraction data did not permit an unambiguous determination of this distance and a redetermination of this structure by x-ray crystallography or other methods is called for. In accord with a previous study,<sup>11</sup> we predict that the axial bond length is about 1.815 Å, close to that of the equatorial I-F bonds.

(viii): The observed structures and bonding in these iodine fluorides and oxofluorides are in accord with previously proposed bonding models.<sup>3,9</sup> Based on these models, the oxygen-iodine  $\sigma$ -bonds and the free valence electron pairs of iodine seek high  $s$  character by utilizing  $sp^n$  orbitals of the iodine atom, while the remaining fluorine ligands preferentially form highly ionic, multi-center bonds.<sup>3,9,42-44</sup>

## Conclusions

The fluoride ion acceptor properties of *cis*- $\text{IO}_2\text{F}_4^-$  and *trans*- $\text{IO}_2\text{F}_4^-$  have been studied. Because of an expected large activation energy barrier in a *cis*- $\text{IO}_2\text{F}_4^-$  /  $\text{F}^-$  adduct toward rearrangement to the energetically favored  $D_{5h}$  *trans*- $\text{IO}_2\text{F}_5^{2-}$  structure, only the *trans*- $\text{IO}_2\text{F}_4^-$  anion acts as a fluoride ion acceptor. The resulting novel *trans*- $\text{IO}_2\text{F}_5^{2-}$  anion has been isolated and characterized, and is presently the only known main-group  $\text{AO}_2\text{F}_5^{n-}$  species. Based on its

vibrational spectra and electronic structure calculations, the  $\text{IO}_2\text{F}_5^{2-}$  anion has the pentagonal-bipyramidal geometry preferred by main-group fluorides and oxofluorides with CN 7. An analysis of the calculated structures of six- and seven-coordinate iodine fluorides and oxofluorides reveals systematic trends that are dominated by changes in the ionicity of the I-F bonds due to the formal ionic charges of the species and the oxidation states of the central atom.

### Acknowledgements

We thank the donors of the Petroleum Research Fund, administered by the American Chemical Society, for support of this work under ACS-PRF No. 28284-AC3 (G.J.S.). We also thank the National Science Foundation for the award of a NATO Postdoctoral Fellowship (W.J.C.). The work at USC was financially supported by the National Science Foundation and that at Edwards by the Air Force Office of Scientific Research and the Defense Advanced Research Projects Agency. One of us (M.G.) thanks the Ontario Ministry of Education and the Richard Fuller and James A. Morrison Memorial Funds for the award of graduate scholarships. A part of the work at PNL was supported by the Department of Energy. We thank Dr. Ross Wagner for his help with the preparation of some starting materials and Dr. Robert Syvret for his preparation of the  $\text{IO}_2\text{F}_3$  sample.

## References

\*Authors to whom correspondence should be addressed. E-mail addresses:

karl.christe@edwards.af.mil; schrobil@mcmil.cif.mcmaster.ca; david.dixon@pnl.gov.

<sup>^</sup>Loker Hydrocarbon Research Institute

<sup>†</sup>Air Force Research Laboratory

<sup>‡</sup>McMaster University

<sup>§</sup>Pacific Northwest National Laboratory

<sup>¶</sup> Present address: Department of Chemistry and Biochemistry, The University of Lethbridge, Lethbridge, Alberta, T1K 3M4, Canada.

- (1) Kepert, D. *Inorganic Stereochemistry*; Springer: Berlin, 1982.
- (2) Gillespie, R. J.; Hargittai, I. *The VSEPR Model of Molecular Geometry*: Allyn and Bacon, A Division of Simon & Schuster, Inc.: Needham Heights, MA, 1991; and Gillespie, R. J.; Popelier, P. L. A. *Chemical Bonding and Molecular Geometry: from Lewis to Electron Densities*; Oxford University Press, 2001.
- (3) Christe, K. O.; Curtis, E. C.; Dixon, D. A.; Mercier, H. P. A.; Sanders, J. C. P.; Schrobilgen, G. J.; Wilson, W. W. *Inorganic Fluorine Chemistry Toward the 21st Century*, ACS Symposium Series 555, American Chemical Society, Washington, DC, 1994, p 66.
- (4) Seppelt, K. *Inorganic Fluorine Chemistry Toward the 21st Century*, ACS Symposium Series 555, American Chemical Society, Washington, DC, 1994, p 56.
- (5) Christe, K. O.; Curtis, E. C.; Dixon, D. A. *J. Am. Chem. Soc.* **1993**, *115*, 1520.
- (6) Christe, K. O.; Dixon, D. A.; Sanders, J. C. P.; Schrobilgen, G. J.; Wilson, W. W. *J.*

- Am. Chem. Soc.* **1993**, *115*, 9461.
- (7) Christe, K. O.; Curtis, E. C.; Dixon, D. A. *J. Am. Chem. Soc.* **1993**, *115*, 9655.
- (8) Drake, G. W.; Dixon, D. A.; Sheehy, J. A.; Boatz, J. A.; Christe, K. O. *J. Am. Chem. Soc.* **1998**, *120*, 8392.
- (9) Christe, K. O.; Curtis, E. C.; Dixon, D. A.; Mercier, H. P. A.; Sanders, J. C. P.; Schrobilgen, G. J. *J. Am. Chem. Soc.* **1991**, *113*, 3351.
- (10) Christe, K. O.; Wilson, W. W.; Drake, G. W.; Dixon, D. A.; Boatz, J. A.; Gnan, R. *Z. J. Am. Chem. Soc.* **1998**, *120*, 4711.
- (11) Christe, K. O.; Dixon, D. A.; Mahjoub, A. R.; Mercier, H. P. A.; Sanders, J. C. P.; Seppelt, K.; Schrobilgen, G. J.; Wilson, W. W. *J. Am. Chem. Soc.* **1993**, *115*, 2696.
- (12) Christe, K. O.; Dixon, D. A.; Sanders, J. C. P.; Schrobilgen, G. J.; Wilson, W. W. *Inorg. Chem.* **1993**, *32*, 4089.
- (13) Christe, K. O.; Dixon, D. A.; Sanders, J. C. P.; Schrobilgen, G. J.; Tsai, S. S., Wilson, W. W. *Inorg. Chem.* **1995**, *34*, 1868.
- (14) Christe, K. O.; Wilson, W. W.; Dixon, D. A.; Boatz, J. A. *J. Am. Chem. Soc.* **1999**, *121*, 3382.
- (15) Christe, K. O.; Wilson, R. D.; Schack, C. J. *Inorg. Synth.* **1986**, *24*, 3.
- (16) (a) Christe, K. O.; Wilson, W. W.; Schack, C. J. *J. Fluorine Chem.* **1978**, *11*, 71; (b) Winfield, J. M. *J. Fluorine Chem.* **1984**, *25*, 91; (c) Emara, A. A. A.; Schrobilgen, G. *J. Inorg. Chem.* **1992**, *31*, 1323.
- (17) Christe, K. O.; Wilson, W. W.; Wilson, R. D.; Bau, R.; Feng, J.-a. *J. Am. Chem. Soc.* **1990**, *112*, 7619.
- (18) Engelbrecht, A.; Peterfy, P.; Schandara, E. Z. *Anorg. Allg. Chem.* **1971**, *384*, 202.
- (19) Wagner, R. I.; Bau, R.; Gnan, R. Z.; Jones, P. F.; Christe, K. O. *Inorg. Chem.* **1997**,

- 36, 2564.
- (20) Christe, K. O.; Wilson, R. D.; Schack, C. J. *Inorg. Chem.* **1981**, *20*, 2104.
- (21) Christe, K. O.; Schack, C. J.; Wilson, R. D.; *Inorg. Chem.* **1977**, *16*, 849.
- (22) (a) Parr, R. G.; Yang, W. *Density Functional Theory of Atoms and Molecules*. Oxford University Press, New York, **1989**; (b) Labanowski, J.; Andzelm, J., Eds. *Density Functional Methods in Chemistry*. Springer Verlag, New York, **1991**; (c) Ziegler, T. *Chem. Rev.* **1991**, *91*, 651; (d) Salahub, D. R. In *Ab Initio Methods in Quantum Chemistry -II*, Lawley, K. P., Ed. J. Wiley & Sons, New York. p. 447, **1987**; (e) Jones, R.O., Gunnarsson, O. *Rev. Mod. Phys.* **1989**, *61*, 689.
- (23) Vosko, S. J.; Wilk, L.; Nusair, W. *Can. J. Phys.* **1980**, *58*, 1200. (Keyword = SVWN5 in Gaussian 98).
- (24) (a) Hirst, D.M. "A Computational Approach to Chemistry" *Blackwell Scientific*, Oxford (1990); (b) Grant, G. H.; Richards, W.G. "Computational Chemistry" Oxford University Press, Oxford (1995); (c) Hehre, W.J.; Radom, L.; Schleyer, P.vR.; Pople, J.A. "Ab Initio Molecular Orbital Theory" John Wiley and Sons, New York (1986).
- (25) Godbout, N.; Salahub, D.R.; Andzelm, J.; Wimmer, E. *Can. J. Chem.* **1992**, *70*, 560. Basis sets were obtained from the Extensible Computational Chemistry Environment Basis Set Database developed in and distributed by the Molecular Science Computing Facility, William R. Wiley Environmental and Molecular Sciences Laboratory, Pacific Northwest National Laboratory.  
<http://www.emsl.pnl.gov:2080/forms/basisform.html>.
- (26) Dunning, T.H., Jr.; Hay, P.J. in *Methods of Electronic Structure Theory*, Schaefer, H.F., III, Ed., Plenum Press: New York, **1977**, Ch. 1.
- (27) Hay, P.J.; Wadt, W. R. *J. Chem. Phys.* **1985**, *82*, 270, 284, 299.

- (28) (a) Andzelm, J.; Wimmer, E.; Salahub, D. R. in *The Challenge of d and f Electrons: Theory and Computation*; Salahub, D. R.; Zerner, M. C., Eds.; ACS Symposium Series, No. 394, American Chemical Society: Washington D. C., 1989; p228. (b) Andzelm, J. in *Density Functional Theory in Chemistry*; Labanowski, J.; Andzelm, J., Eds.; Springer-Verlag: New York, 1991, p 155. (c) Andzelm, J. W.; Wimmer, E. *J. Chem. Phys.* **1992**, *96*, 1280.
- (29) Frisch, M. J.; Trucks, G. W.; Schlegel, H. B.; Scuseria, G. E.; Robb, M. A.; Cheeseman, J. R.; Zakrzewski, V. G.; Petersson, G. A.; Montgomery, J. A., Jr.; Stratmann, R. E.; Burant, J. C.; Dapprich, S.; Millam, J. M.; Daniels, A. D.; Kudin, K. N.; Strain, M. C.; Farkas, O.; Tomasi, J.; Barone, V.; Cossi, M.; Cammi, R.; Mennucci, B.; Pomelli, C.; Adamo, C.; Clifford, S.; Ochterski, J.; Petersson, G. A.; Ayala, P. Y.; Cui, Q.; Morokuma, K.; Malick, D. K.; Rabuck, A. D.; Raghavachari, K.; Foresman, J. B.; Cioslowski, J.; Ortiz, J. V.; Stefanov, B. B.; Liu, G.; Liashenko, A.; Piskorz, P.; Komaromi, I.; Gomperts, R.; Martin, R. L.; Fox, D. J.; Keith, T. A.; Al-Laham, M. A.; Peng, C. Y.; Nanayakkara, A.; Gonzalez, C.; Challacombe, M.; Gill, P. M. W.; Johnson, B. G.; Chen, W.; Wong, M. W.; Andreas, J. L.; Head-Gordon, M.; Replogle, E. S.; Pople, J. A. *Gaussian 98*, A.7, Gaussian, Inc. Pittsburg PA, 1998.
- (30) BMATRIX Version 2.0; Kormonicki, A.; Polyatomics Research Institute: Palo Alto, CA, 1996.
- (31) Gillespie, R. J.; Robinson, E. A. *Angew. Chem. Int. Ed. Engl.* **1996**, *35*, 495.
- (32) Berry, R. S. *J. Chem. Phys.* **1960**, *32*, 933.
- (33) Gillespie, R. J.; Krasznai, J. P. *Inorg. Chem.* **1977**, *16*, 1384.
- (34) Gerken, M. Ph. D. Thesis, McMaster University, Hamilton, ONT. 2001.

- (35) Berg, R. W. *Spectrochim. Acta, Part A* **1978**, 34A, 655.
- (36) Zachariasen, W. H. *Acta Crystallogr.* **1954**, 7, 783.
- (37) Nguyen-Quy-Dao, *Bull. Soc. Chim. Fr.* **1968**, 3976.
- (38) Nakamoto, K. *Infrared and Raman Spectra of Inorganic and Coordination Compounds, Part A*; John Wiley and Sons, Inc. New York, Fifth Ed. 1997, p 228.
- (39) Christe, K. O.; Dixon, D. A.; Mack, H. G.; Oberhammer, H.; Pagelot, A.; Sanders, J. P. G.; Schrobilgen, G. J. *J. Am. Chem. Soc.* **1993**, 115, 11279.
- (40) Mahjoub, A.-R.; Seppelt, K. *Angew. Chem., Int. Ed. Engl.* **1991**, 30, 323.
- (41) Mahjoub, A.-R.; Drews, T.; Seppelt, K. *Angew. Chem., Int. Ed. Engl.* **1992**, 31, 1036.
- (42) Pimentel, G. C. *J. Chem. Phys.* **1951**, 19, 446.
- (43) Hach, R. J.; Rundle, R. E. *J. Am. Chem. Soc.* **1951**, 73, 4321.
- (44) Rundle, R. E. *J. Am. Chem. Soc.* **1963**, 85, 112.
- (45) Bartell, L. S.; Clippard, F. B.; Jacob, E. J. *Inorg. Chem.* **1976**, 15, 3009.

**Table 1.** Observed and Calculated Vibrational Spectra of the *trans*-IO<sub>2</sub>F<sub>5</sub><sup>2-</sup> Anion and their Assignment in Point Group D<sub>5h</sub>

assign (activity)	approx mode description	obsd freq, cm <sup>-1</sup> Raman <sup>a,b</sup>	(rel intensity) for [N(CH <sub>3</sub> ) <sub>4</sub> ] <sub>2</sub> [IO <sub>2</sub> F <sub>5</sub> ] <sup>c,d</sup> Infrared	scaled <sup>f</sup> calcd freq, cm <sup>-1</sup> (Ir, Ra intens)	LDFI/DZVP HF/ECP/DZVP
A <sub>1</sub> ' (Ra)	ν <sub>1</sub> , ν sym IO <sub>2</sub>	789 [100]	-	781(0) [37]	776 (0) [43]
	ν <sub>2</sub> , ν sym IF <sub>5</sub>	517 [57]	-	505 (0) [29]	505 (0) [27]
A <sub>2</sub> " (IR)	ν <sub>3</sub> , ν as IO <sub>2</sub>	-	847 s <sup>e</sup>	856 (150) [0]	861 (90) [0]
	ν <sub>4</sub> , δ umbrella IF <sub>5</sub>	-	330 m, sh <sup>e</sup>	338 (40) [0]	352 (86) [0]
E <sub>1</sub> ' (IR)	ν <sub>5</sub> , ν as IF <sub>5</sub>	-	490 vs	537 (591) [0]	503 (808) [0]
	ν <sub>6</sub> , δ scissoring IO <sub>2</sub>	-	390 s	389(97) [0]	391 (291) [0]
	ν <sub>7</sub> , δ as IF <sub>5</sub> in plane	-	not obsd	244 (0) [0]	251 (0) [0]
E <sub>1</sub> " (Ra)	ν <sub>8</sub> , δ rock IO <sub>2</sub>	368 [57]	-	340 (0) [13]	346 (0) [14]
E <sub>2</sub> ' (Ra)	ν <sub>9</sub> , ν as IF <sub>5</sub>	not obsd <sup>e</sup>	-	449 (0) [4]	442 (0) [0.6]
	ν <sub>10</sub> , δ scissoring IF <sub>5</sub>	395 [26] <sup>e</sup>	-	393 (0) [7]	392 (0) [3.8]
E <sub>2</sub> " (i.a.)	ν <sub>11</sub> , δ puckering IF <sub>5</sub>	-	-	158 (0) [0]	176 (0) [0]

<sup>a</sup> Spectrum recorded on microcrystalline solid in a Pyrex glass capillary at -113 °C using the 514.5-nm excitation. <sup>b</sup> The N(CH<sub>3</sub>)<sub>4</sub><sup>+</sup> cation modes were observed at 380 (11), ν<sub>8</sub>(E); 457 (13), ν<sub>19</sub>(F<sub>2</sub>); 752 (35), ν<sub>3</sub>(A<sub>1</sub>); 953 (22), ν<sub>18</sub>(F<sub>2</sub>); 1187 (3), ν<sub>1</sub>(E); 1294 (3), ν<sub>17</sub>(F<sub>2</sub>); 1418 (5), ν<sub>16</sub>(F<sub>2</sub>); 1465 sh, ν<sub>2</sub>(A<sub>1</sub>); 1476 (31), ν<sub>6</sub>(E); 2818 (4), 2828 (5), 2836 (5), 2899 sh, 2934 (16), 2970 (25), 2995 (15), 3038 (33) cm<sup>-1</sup>, ν<sub>CH3</sub> and binary bands (see refs 17 and 33). The *cis*-IO<sub>2</sub>F<sub>4</sub><sup>-</sup> anion modes were observed at 209 (1), 331 (14), 356(3)sh, bending modes;

395(26),  $\nu_4(A_1)$ ; 567 (7),  $\nu_3(A_1)$ ; 608 (26),  $\nu_2(A_1)$ ; 854 (31),  $\nu_1(A_1)$ ; 871 (5),  $\nu_{12}(B_2)$  (see ref 20 and Table 3). Bands arising from residual  $\text{CH}_3\text{CN}$  were observed at 916 (7),  $\nu_4(A_1)$ ; 1378 (1),  $\nu_3(A_1)$ ; 2247 (14),  $\nu_2(A_1)$ ; 2944 (16)  $\text{cm}^{-1}$ ,  $\nu_1(A_1)$ .<sup>d</sup> The  $\text{N}(\text{CH}_3)_4^+$  cation modes were observed at 462 sh,  $\nu_{19}(F_2)$ ; 922 w,  $2\nu_{19}$ ; 955 vs,  $\nu_{18}(F_2)$ ; 1257 mw, 1288 mw,  $\nu_{17}(F_2)$ ; 1420 m,  $\nu_{16}(F_2)$ ; 1497 s,  $\nu_{15}(F_2)$ ; 1774 w, br, 1943 w, br, 2340 w, 2362 w, 2499 w, 2589 w, 2998 m, 3046 s, 3411 vw, 3493 vw  $\text{cm}^{-1}$ ,  $\nu_{\text{CH}_3}$  and binary bands (see refs 17 and 35). The  $\text{cis-IO}_2\text{F}_4^-$  anion modes were observed at 354 vs; 367 vs,  $\nu_5(A_1)$ ; 564 sh,  $\nu_3(A_1)$ ; 620 vs, br,  $\nu_2(A_1)$  and  $\nu_9(B_1)$ ; 847 vs,  $\nu_1(A_1)$ ; 871 vs,  $\nu_{12}(B_2)$  (see ref 20 and Table 3).<sup>e</sup> These  $\text{IO}_2\text{F}_5^{2-}$  anion bands overlap with bands of the  $\text{cis-IO}_2\text{F}_4^-$  anion.<sup>f</sup> The following empirical scaling factors were used to obtain the best fit with the observed frequencies: LDFT, I-O stretching modes, 1.1081; HF, I-O stretching modes, 1.0436; remaining modes, 0.9388.<sup>g</sup> Obscured by the  $457 \text{ cm}^{-1}$  Raman band of  $\text{N}(\text{CH}_3)_4^+$ .

Table 2. Comparison of the Vibrational Frequencies of the Pentagonal Planar IF<sub>5</sub> part in *trans*-IO<sub>2</sub>F<sub>3</sub> with those of IF<sub>7</sub>, IOF<sub>6</sub>, IOF<sub>5</sub><sup>2-</sup>, and IF<sub>5</sub><sup>2-</sup> in Point Group C<sub>5v</sub>

assign	approx mode description	+VII	+VII	+VII	+V	+III
		IF <sub>7</sub> [5]	replacmt. of F by O IOF <sub>6</sub> [11]	IO <sub>2</sub> F <sub>3</sub> <sup>2-</sup>	replacmt. of O by free valence el. pair IOF <sub>5</sub> <sup>2-</sup> [14]	IF <sub>5</sub> <sup>2-</sup> [10]
A <sub>1</sub>	v sym IF <sub>5</sub>	635	584	517	485	474
	δ umbrella IF <sub>5</sub>	365	359	330	289	[307] <sup>a</sup>
E <sub>1</sub>	v asym IF <sub>5</sub>	670	585	490	334	335
	δ as IF <sub>5</sub> in plane	425	405	[250]	254	245
E <sub>2</sub>	v asym IF <sub>5</sub>	596	530	[450]	367/355	339/325
	δ scissoring IF <sub>5</sub>	510	457	395	409	396
	δ puckering IF <sub>5</sub>	[68]	[59]	[160]	[115]	[100]

<sup>a</sup> Values in brackets are calculated frequencies.

Table 3. Observed and Calculated Vibrational Spectra of the *cis*-IO<sub>2</sub>F<sub>4</sub> Anion and their Assignment in Point Group C<sub>2v</sub>

assign (activity)	approx mode description	obsd freq, cm <sup>-1</sup> (rel intensity)		scaled <sup>b</sup> calcd freq, cm <sup>-1</sup> (Ir, Ra intens)				
		N(CH <sub>3</sub> ) <sub>4</sub> IO <sub>2</sub> F <sub>4</sub>	Raman (solid) Infrared (solid)	CsIO <sub>2</sub> F <sub>4</sub> <sup>a</sup>	LDFI/DZVP HF/ECP/DZVP			
A <sub>1</sub> (IR,Ra)	v <sub>1</sub> , v sym IO <sub>2</sub>	847 [100]	844 s	856 [100]	855 vs	851 [90] p	863 (73) [22]	868 (87) [29.9]
	v <sub>2</sub> , sym comb of v sym IF <sub>2eq</sub> and v sym IF <sub>2ax</sub>	608 [85]	605 s	605 [98]	600 vs, br	609 [100] p	593 (106) [30]	612 (134) [26.1]
	v <sub>3</sub> , asym comb of v sym IF <sub>2eq</sub> and v sym IF <sub>2ax</sub>	560 [24]	565 sh	552 sh	560 vw	540 [100] p	542 (0) [1.1]	556 (6) [6.3]
	v <sub>4</sub> , δ sciss IO <sub>2</sub>	394 [15]	393 vw	394 [34]	395 sh	— <sup>c</sup>	377 (0) [4.6]	383 (20) [2.2]
	v <sub>5</sub> , sym comb of δ sciss IF <sub>2eq</sub> and δ sciss IF <sub>2ax</sub>	370 [20]	370 s	369 [30]	364 s	355 sh <sup>c</sup>	366 (41) [3.2]	364 (92) [4.4]
	v <sub>6</sub> , asym comb of δ sciss IF <sub>2eq</sub> and δ sym IF <sub>2ax</sub>	207 [3]		210 [0.5]			208 (0) [0.13]	227 (0.1) [0.1]
A <sub>2</sub> (-,Ra)	v <sub>7</sub> , torsion IO <sub>2</sub>	330 [38]	329 vw	332 [65]	328 w	335 sh	294 (0) [3.3]	320 (0) [3.4]
	v <sub>8</sub> , torsion IF <sub>2eq</sub>	610 <sup>d</sup>	613 vs				172 (0) [0.1]	196 (0) [0.1]
B <sub>1</sub> (IR,Ra)	v <sub>9</sub> , v as IF <sub>2ax</sub>				600 vs, br		614 (205) [1.1]	615 (280) [1.3]

$\nu_{10}$ , $\delta$ rock IO <sub>2</sub>	353 s	350 s	341 (35) [1.3]	360 (94) [0.9]
$\nu_{11}$ , $\delta$ rock IF <sub>2eq</sub>	329 vw	328 w	287 (0) [4.4]	321 (1) [2.5]
B <sub>2</sub> (IR,Ra) $\nu_{12}$ , $\nu$ as IO <sub>2</sub>	868 vs	875 vs	884 (114) [6.7]	885 (122) [9.0]
$\nu_{13}$ , $\nu$ as IF <sub>2eq</sub>	555 m	550 mw	551 (32) [3.3]	533 (41) [1.6]
$\nu_{14}$ , sym comb of $\delta$ sciss	370 s	364 s	365 (48) [0.70]	371 (115) [0.6]
OIF <sub>e</sub> and FIF <sub>ax</sub>				
$\nu_{15}$ , asym comb of $\delta$ sciss			209 (0) [0.002]	227 (0) [0]
OIF <sub>e</sub> and FIF <sub>ax</sub>				

<sup>a</sup>Data from ref 20. <sup>b</sup>Empirical scaling factors of 1.06 and 1.122 were used for the LDF $\Gamma$  stretching and deformation modes, respectively, to maximize the fit between observed and calculated frequencies; for the HH/ECP frequencies, scaling factors of 1.0, 0.9238, and 0.8615 were used for the IO stretching, the IF stretching, and the deformations modes, respectively. <sup>c</sup>Interference from a strong solvent band. <sup>d</sup>Intensities were omitted because of coincidences with other modes which contribute more strongly to the intensity.

**Table 4.** Calculated Unscaled and Predicted Geometries for  $\text{IO}_2\text{F}_5^{2-}$ 

	HF/ECP/DZVP	LDFT/DZVP	predicted
R(I-F), Å	1.948	2.057	1.97
R(I-O), Å	1.751	1.824	1.78
$\angle$ F-I-O, deg	90	90	90
$\angle$ F-I-F, deg	72	72	72

**Table 5.** Symmetry Force Constants<sup>a</sup> and Potential Energy Distribution<sup>b</sup> of  $D_{5h}$   $\text{IO}_2\text{F}_5^{2-}$  Calculated from the Scaled<sup>c</sup> LDFT/DZVP Second Derivatives

	freq, $\text{cm}^{-1}$		sym force constants	PED
	obsd	calcd		
$A_1'$	789	781	$F_{11} = 5.74$	100 (1)
			$F_{12} = 0.128$	
$A_2''$	517	505	$F_{22} = 2.86$	100 (2)
	847	856	$F_{33} = 5.54$	95 (3)
$E_1'$			$F_{34} = 0.225$	
	330	338	$F_{44} = 1.70$	100 (4)
$E_1''$	490	537	$F_{55} = 2.45$	90 (5), 7 (6), 2(8)
			$F_{56} = -0.521$	
			$F_{57} = 0.195$	
	390	389	$F_{66} = 2.45$	78 (6), 21 (7)
$E_2'$			$F_{67} = -0.450$	
	-	244	$F_{77} = 1.18$	58 (6), 41 (7)
$E_1''$	368	340	$F_{88} = 0.947$	100 (8)
$E_2''$	-	449	$F_{99} = 2.18$	88 (9), 12 (10)
			$F_{9,10} = 0.194$	
$E_2''$	395	393	$F_{10,10} = 2.11$	84 (10), 15 (9)
	-	158	$F_{11,11} = 0.598$	100 (11)

<sup>a</sup> Stretching constants in  $\text{mdyn}/\text{\AA}$ , deformation constants in  $\text{mdyn}\text{\AA}/\text{rad}^2$ , and stretch-bend interactions constants in  $\text{mdyn}/\text{rad}$ . The force constants were scaled with the square of the scaling factors used for the corresponding frequencies. <sup>b</sup> PED in percent; symmetry coordinates:  $S_1 = \nu$  sym  $\text{IO}_2$ ;  $S_2 = \nu$  sym  $\text{IF}_5$ ;  $S_3 = \nu$  asym  $\text{IO}_2$ ;  $S_4 = \delta$  umbrella  $\text{IF}_5$ ;  $S_5 = \nu$  asym  $\text{IF}_5$ ;  $S_6 = \delta$  scissoring  $\text{IO}_2$ ;  $S_7 = \delta$  asym  $\text{IF}_5$  in plane;  $S_8 = \delta$  rock  $\text{IO}_2$ ;  $S_9 = \nu$  asym  $\text{IF}_5$ ;  $S_{10} = \delta$  scissoring  $\text{IF}_5$ ;  $S_{11} = \delta$  puckering  $\text{IF}_5$ .

**Table 6.** Geometry and Unscaled Vibrational Frequencies (Infrared Intensities) of the *cis*-isomer of  $\text{IO}_2\text{F}_5^{2-}$  Calculated at the LDFT/DZVP Level of Theory in Point Group  $C_s$

freq, $\text{cm}^{-1}$ (IR intens)	geometry	
a' 780.6 (123)	R(I-O2)	1.846
734.5 (86)	R(I-O3)	1.830
477.0 (135)	R(I-F4)	2.038
439.4 (30)	R(I-F5)	2.100
422.3 (0.25)	R(I-F7)	2.066
372.9 (5.7)		
337.4 (66)	$\angle(\text{O2-I-O3})$	110.0
323.3 (37)	$\angle(\text{O2-I-F4})$	85.2
303.9 (4.4)	$\angle(\text{O2-I-F5})$	78.0
224.2 (0.03)	$\angle(\text{O3-I-F5})$	89.6
91.3 (0)	$\angle(\text{O3-I-F7})$	91.2
	$\angle(\text{F4-I-F5})$	93.7
a" 455.5 (258)	$\angle(\text{F4-I-F7})$	76.3
423.0 (2.2)	$\angle(\text{F5-I-F7})$	68.4
367.9 (72)	$\angle(\text{F7-I-F8})$	69.1
350.3 (1.3)		
282.3 (0.08)		
205.7 (0.03)		
28.5 (0.08)		

## Diagram Captions

**Figure 1.** The Raman spectrum of  $[\text{N}(\text{CH}_3)_4]_2[\text{IO}_2\text{F}_5]$  containing about 25 weight % of  $[\text{N}(\text{CH}_3)_4][\text{cis-IO}_2\text{F}_4]$ , recorded at  $-113\text{ }^\circ\text{C}$  using 514.5 nm excitation. The *trans-IO*<sub>2</sub>F<sub>5</sub><sup>2-</sup>, *cis-IO*<sub>2</sub>F<sub>4</sub><sup>-</sup>, and N(CH<sub>3</sub>)<sub>4</sub> bands are indicated by ‡, \*, and • respectively.

**Figure 2.** *D*<sub>5h</sub> geometry of the *trans-IO*<sub>2</sub>F<sub>5</sub><sup>2-</sup> anion.

**Figure 3.** Geometries of the hexacoordinated *IO*<sub>2</sub>F<sub>4</sub><sup>-</sup>, *IOF*<sub>4</sub><sup>-</sup>, *IF*<sub>4</sub><sup>-</sup>, *IOF*<sub>5</sub>, *IF*<sub>5</sub>, and *IF*<sub>6</sub><sup>+</sup> ions and molecules, calculated at the HF/ECP/DZVP level of theory. The calculated bond lengths and bond angles are given in bold and regular fonts, respectively, and the experimentally observed values are shown in brackets.

**Figure 4.** Geometries of the heptacoordinated *IO*<sub>2</sub>F<sub>5</sub><sup>2-</sup>, *IOF*<sub>5</sub><sup>2-</sup>, *IF*<sub>5</sub><sup>2-</sup>, *IOF*<sub>6</sub><sup>-</sup>, *IF*<sub>6</sub><sup>-</sup>, and *IF*<sub>7</sub> ions and molecules, calculated at the HF/ECP/DZVP level of theory. The calculated bond lengths and bond angles are given in bold and regular fonts, respectively, and the experimentally observed values are shown in brackets.

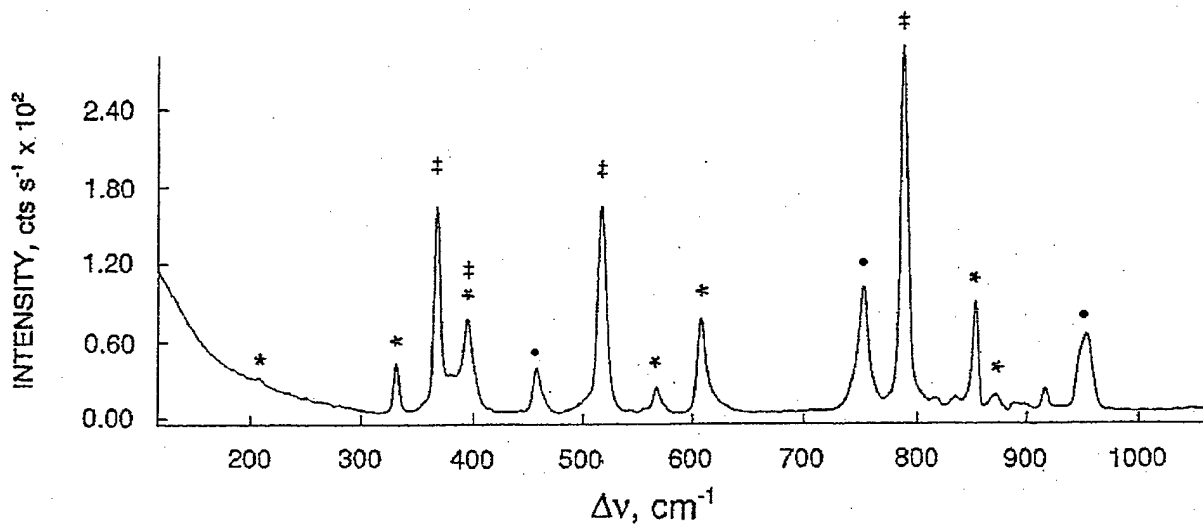
**Figure 5.** Minimum energy structure of *cis-IO*<sub>2</sub>F<sub>5</sub><sup>2-</sup> calculated at the LDFT/DZVP level.

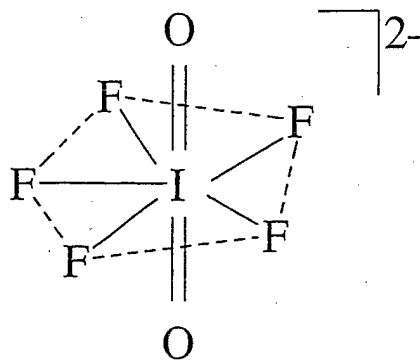
**Figure 6.** Changes of the equatorial I-F bond lengths with increasing formal ion charge and decreasing oxidation state of the central iodine atom. The arrangement of the individual compounds is identical to those in Figures 3 and 4, and the italic and regular numbers represent the hexa- and hepta-coordinated species, respectively.

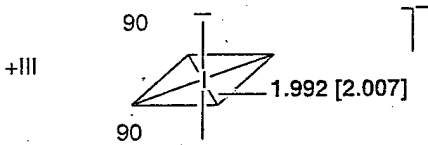
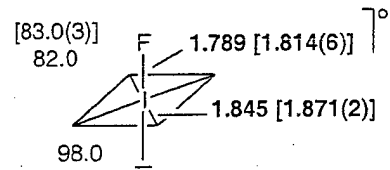
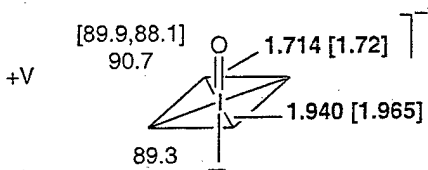
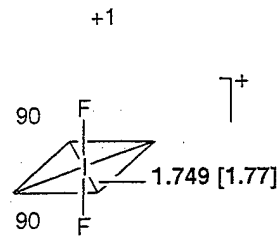
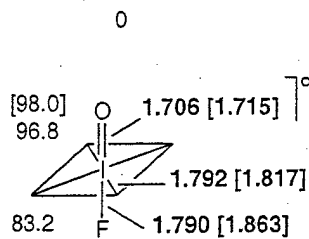
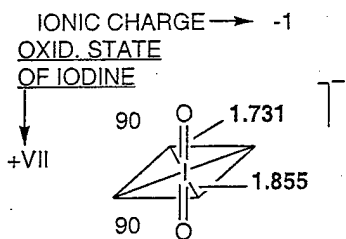
**Figure 7.** Changes of the axial I-F bond lengths with increasing ion charge and decreasing oxidation state of the central iodine atom. Italic and regular font numbers represent the hexa- and hepta-coordinated species, respectively.

**Figure 8.** Changes of the axial I-O bond lengths with increasing ion charge and decreasing oxidation state of the central iodine atom. Italic and regular font numbers repre-

sent the hexa- and hepta-coordinated species, respectively.

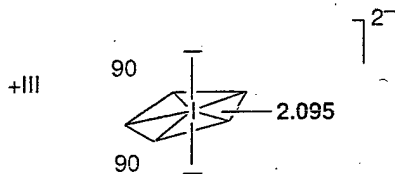
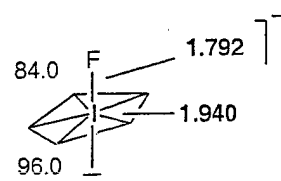
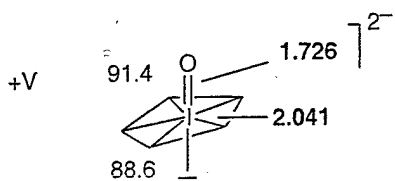
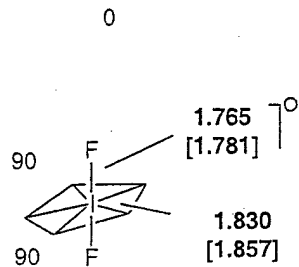
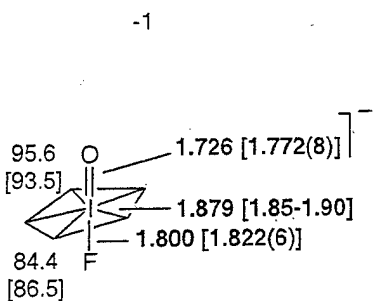
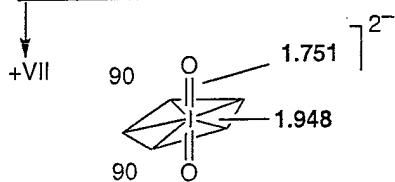




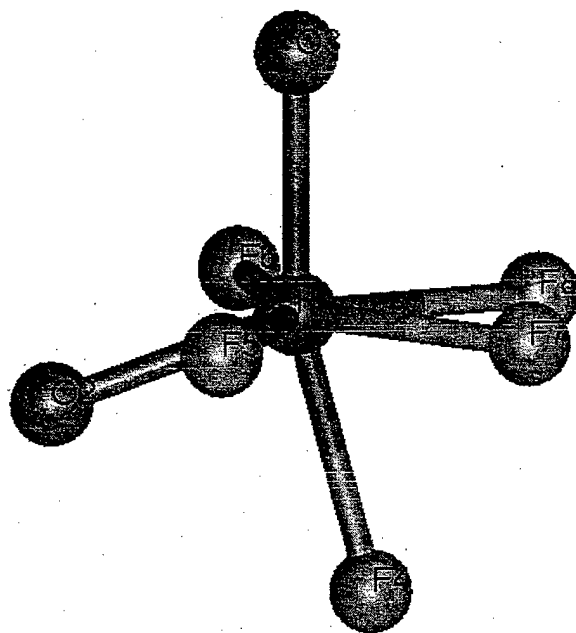


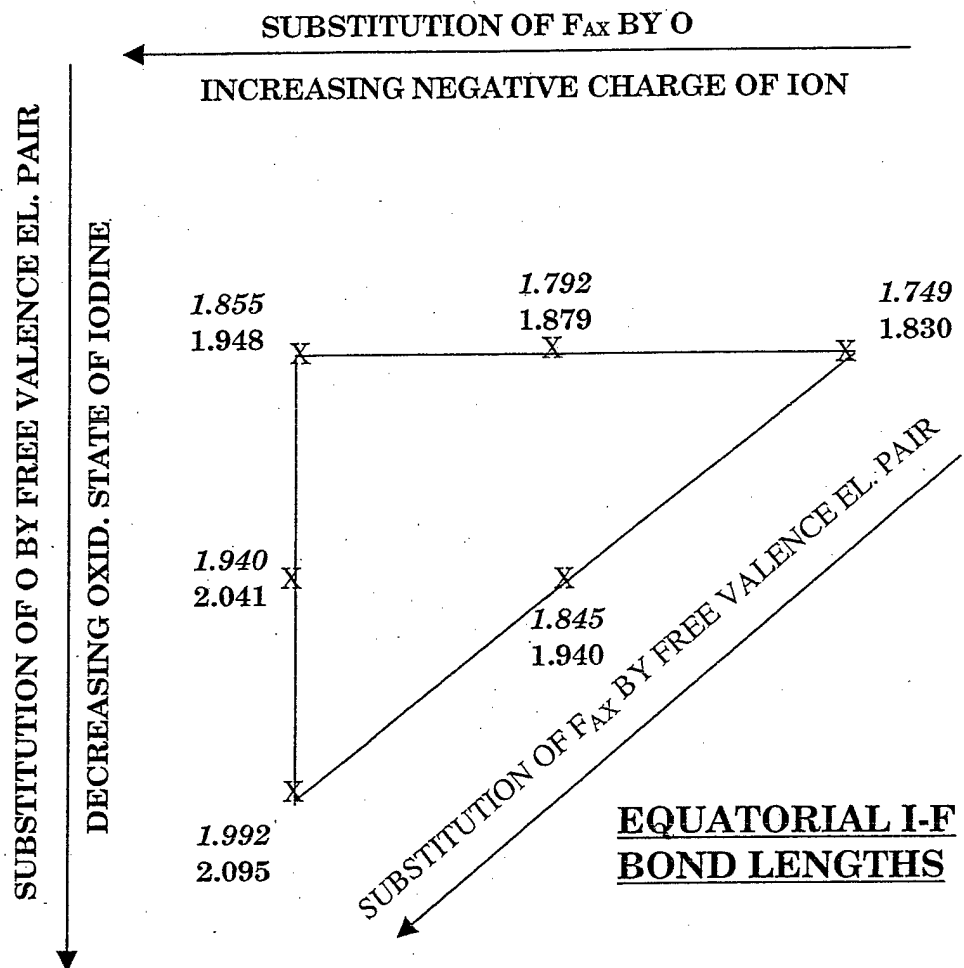
CN 6

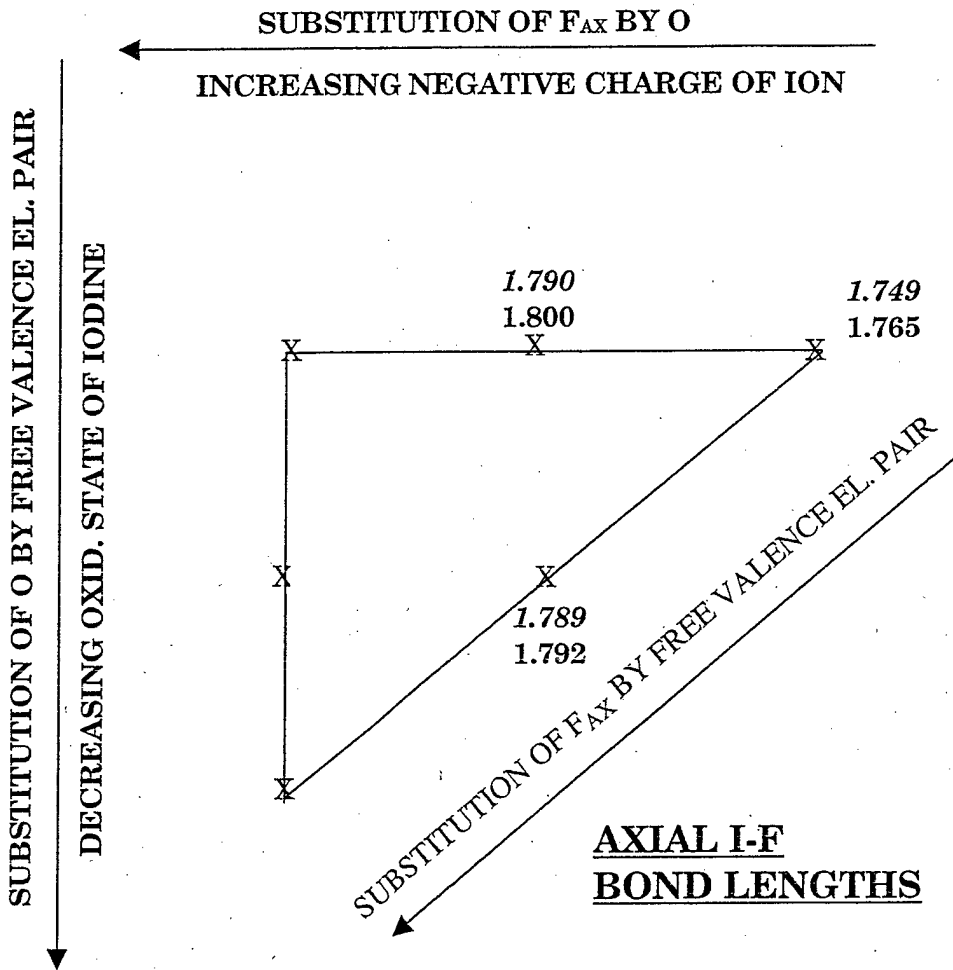
IONIC CHARGE → -2  
 OXID. STATE  
 OF IODINE

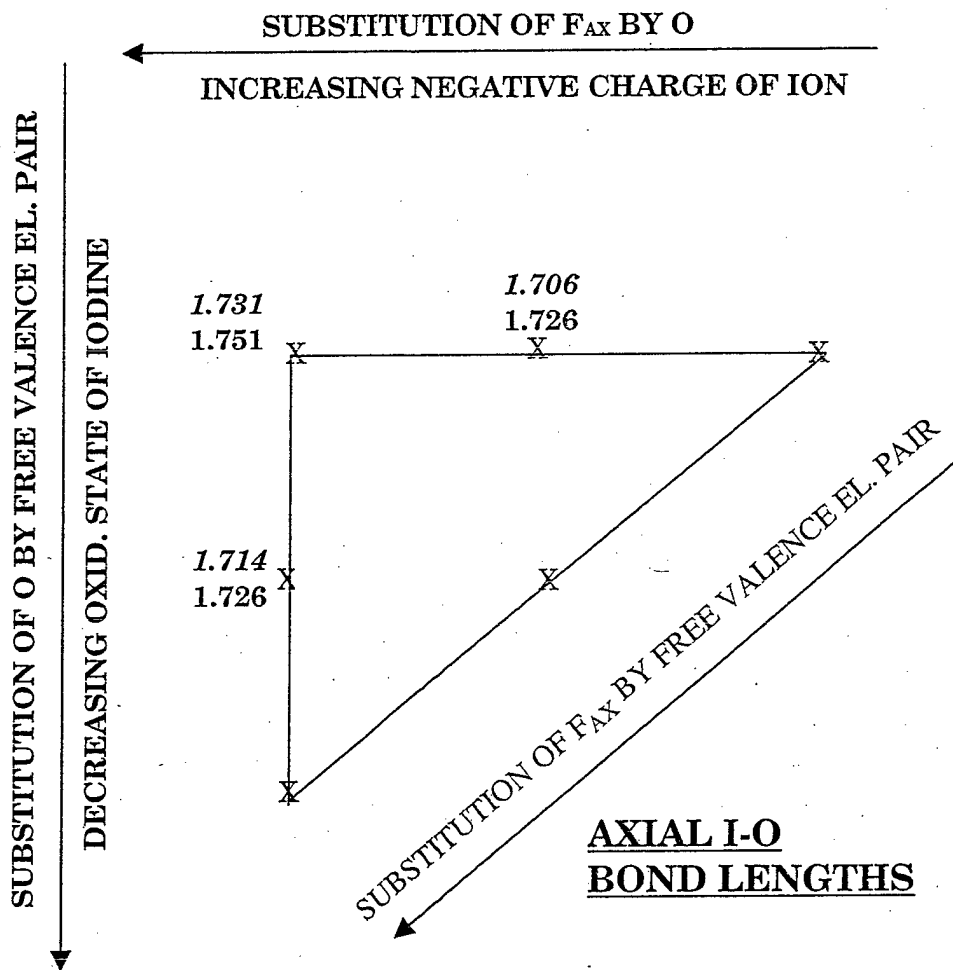


CN 7









## Synthesis and Characterization of the *trans*-IO<sub>2</sub>F<sub>5</sub><sup>2-</sup> Dianion

Jerry A. Boatz, William J. Casteel, Jr., Karl O. Christe,\*

David A. Dixon, Michael Gerken, Robert Z. Gnann,

Helène P. A. Mercier, and Gary J. Schrobilgen\*

